



Performance investigations of nonlinear piezoelectric energy harvesters with a resonant circuit under white Gaussian noises

Tianjun Yu · Sha Zhou

Received: 21 September 2020 / Accepted: 17 December 2020 / Published online: 6 January 2021
© The Author(s), under exclusive licence to Springer Nature B.V. part of Springer Nature 2021

Abstract Vibration-based piezoelectric energy harvesting for powering low-energy consuming electronic equipment has received a great deal of attention in the last decade. Most researches applying deterministic approaches or theory of random vibrations have been concentrated on examining the performance of the piezoelectric energy harvesters with a purely resistive circuit under harmonic or random excitations. Here, the ambient excitations are assumed to be white Gaussian noises, we investigate a nonlinear piezoelectric energy harvester which utilizes a harvesting circuit with both a resistive load and an inductor, based on the fact that previous research has demonstrated that the intentional introduction of an inductor substantially improves the performance of energy harvesting device. Two scenarios, namely the purely inductive circuit and the resistive–inductive circuit, are examined. Exact stationary solution of the output voltage and closed-form expression of the mean square voltage are acquired for the purely inductive circuit. By combining the equivalent linearization

method and the moment method of random process theory, analytical solutions of mean square voltage and averaged power output involving dimensionless parameters of the electromechanical system are derived for the resistive–inductive circuit. The energy conversion efficiency is analyzed by means of energy balance equation. Monte Carlo numerical simulations are implemented to validate the theoretical predictions. Results reveal unique characteristics of the nonlinear vibration systems with a resonant circuit, showing its superiority over the energy harvesters with a purely resistive circuit. The present study provides a paradigm in a simple but effective way to resolve strong electromechanical coupling systems under random excitations.

Keywords Energy harvesting · Random vibration · Electromechanical coupling · Exact stationary solution · Equivalent linearization method · Energy conversion efficiency

T. Yu
Key Laboratory of Dynamics and Control of Flight Vehicle, Ministry of Education and School of Aerospace Engineering, Beijing Institute of Technology, Beijing 100081, China

S. Zhou (✉)
Department of Engineering Mechanics, Zhejiang University, Hangzhou 310027, China
e-mail: lilyzhou191@hotmail.com

1 Introduction

Since a long time ago, humans have started exploring the feasibility of harnessing ambient energy to supply considerable electrical energy by using waterwheels and windmills. Even now, such electromechanical conversion devices are still major power supply way in many remote regions. With the continuous

development of science and technology, compact and scalable electronic devices emerge, such as wireless sensors, portable health monitors, and data transmitters. The common feature of these devices is that the power requirements have been significantly reduced. For instance, the electronic microchips for health monitoring approximately consume an average power of $50 \mu\text{W}$ [1, 2]. It promotes researchers to develop new micropower generators as a scalable continuous energy source for substituting batteries. In practice, unavoidable vibrations reside in diverse mechanical and human body systems, for example, the whirling motion of rotors [3–7], the forced or the parametrically excited vibration of pipes conveying fluid [8–12], aeroelastic response of flexible structures [13–19], the heart pumping and the arterial pulse [20–23]. Vibratory energy harvesting has formed a branch in the field of mechanical engineering, electronics and applied mechanics and is deeply integrated among them.

Vibration-based piezoelectric energy harvesters (PEHs) use the electromechanical coupling effect of piezoelectric crystals experiencing ambient vibrations to produce electric energy that can be simultaneously stored up for supplying power. For the PEHs operating by means of the principle of linear resonance, the frequency bandwidth is usually very narrow. That results in great limitations on the usefulness and applicability of the harvesters. Fortunately, for some natural structures and the precisely designed artificial structures, nonlinearities arising from nonlinear strain–deflection relationships or nonlinear constitutive relations can be easily observed. The introduction of nonlinearities into the innovative design of PEHs has been a widespread concerned topic [24, 25]. Some results have pointed out that elaborately introduced nonlinearity could be beneficial to harvest energy because the harvester's operation bandwidth can be extended [26–32] when compared to the linear device. It is noteworthy that nonlinearity yields non-unique solutions of response for certain frequency domains which are characterized by the presence of coexisting motions, and the nonlinear energy harvesters are not always guaranteed to hold the desired large amplitude resonant state. Actually, the practical operating state is depending on the basins of attraction of the coexisting solutions [33, 34].

Up to now, most of the researches reported regard the ambient vibration exerting on the PEHs has some deterministic form. However, it is an indisputable fact

that most ambient energy is actually distributed over a wide frequency spectrum. In such scenario, researchers need to apply the theory of random processes to describe the ambient excitation and perform the response analysis of harvested power output under the framework of stochastic dynamics [35–37]. For improving the harvester's performance in an actual environment, recently, some research groups have studied the influence of the nonlinearity on the transduction characteristics of nonlinear piezoelectric energy harvesters (NPEHs) with a purely resistive circuit under random excitations [38–42]. Although the merits of the stochastic resonance effect for performance improvement in the bistable harvesters have been reported by McInnes et al. [43], but when only harmonic excitation are considered, researchers examined the performance of a bistable harvester relative to a monostable harvester and their theoretical and experimental results indicated that the bistable configuration did not distinctly show significant enhancement in the power output [44]. Even in the case of white Gaussian excitations, the bistability did not seem to furnish much output power improvement unless the time constant ratio is very small [45, 46]. Recent researches have demonstrated that the performance metrics can be improved by the harvesters with a resonant circuit, comparing with the harvesters with a purely resistive circuit [47–49]. It is worth mentioning that for the energy harvesters with a purely resistive circuit, the recognized principle for improving the output voltage and power by augmenting the displacement response, such as constructing multi-stable energy harvesters, may be invalid when the energy harvesters with a resonant circuit under white Gaussian noises is considered, due to the competitive mechanism between the mechanical degree of freedom and the electrical degree of freedom. To the best of our knowledge, there is still a lack of corresponding analytical strategy for solving the response statistics of strong two-way coupling NPEHs with a resonant circuit under random excitations and energy conversion efficiency is an open issue until now [49–51]. These circumstances motivate us to make this work for understanding the influence of the system parameters with regard to the performance metrics of monostable NPEHs with a resonant circuit.

The rest of this paper is organized as follows: In Sect. 2, a two-degree-of-freedom NPEH model excited by random noises is introduced and its

electromechanical coupling equations are then transformed into a Itô stochastic equation. In Sect. 3, an exact stationary solution of probability density function of voltage output and simple expressions of the mean square values of responses are derived in the purely inductive circuit scenario. In Sect. 4, for the resistive–inductive circuit scenario, with the help of the direct equivalent linearization method and the moment method of random process theory, analytical solutions of the mean square voltage and the averaged power output are derived and the energy conversion efficiency is also attained based on energy balance equation. In Sect. 5, the variation law of the mean square voltage and efficiency (averaged power output) with respect to system parameters is investigated in detail. In Sect. 6, we end this investigation with concluding remarks.

2 Electromechanical model

From the perspective of working principle, the PEHs can be traditionally divided into two categories, namely, inertial harvesters and non-inertial harvesters [50]. In this investigation, we focus on the inertial NPEHs, specifically, ambient vibration energy is harvested by means of a nonlinear mechanical system coupled with a resonant circuit. Considering a stack-type nonlinear piezoelectric device operating in the 33 mode with a resistive–inductive circuit in parallel in the electrical domain; see Fig. 1. The nonlinear

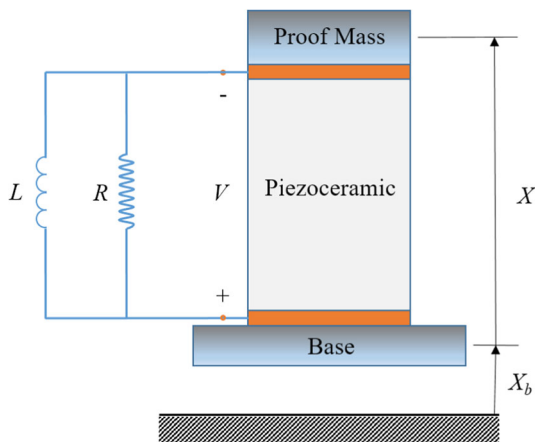


Fig. 1 Schematic diagrams of a piezoelectric energy harvester with a RL resonant circuit

differential equations of such electromechanical coupled model can be written as

$$m\ddot{X}(t) + c\dot{X}(t) + k_lX(t) - \theta V(t) + k_{nl}X(t)^3 = -m\ddot{X}_b(t) \tag{1a}$$

$$C_p\ddot{V}(t) + \theta\ddot{X}(t) + \frac{1}{R}\dot{V}(t) + \frac{1}{L}V(t) = 0 \tag{1b}$$

where the overdot represents the derivative with respect to time t . X and V denote the displacement response of mass m and the voltage response measured across the resistance R , respectively. c is the mechanical damping, θ is the electromechanical coupling, C_p is the capacitance and L is the inductance. k_l and k_{nl} are linear and nonlinear stiffness, respectively. \ddot{X}_b represents the base acceleration which is considered to be a broadband random process.

Introducing the dimensionless transformations and parameters as follows

$$\begin{aligned} \bar{X} &= \frac{X}{l}, \bar{V} = V\sqrt{\frac{C_p}{l^2k_l}}, \tau = t\omega_0 = t\sqrt{\frac{k_l}{m}} \\ \mu &= \frac{c}{m\omega_0}, \alpha = \frac{k_{nl}l^2}{k_l}, \chi = \frac{\theta}{\sqrt{k_lC_p}}, \beta = \frac{1}{\omega_0RC_p}, \gamma = \frac{1}{\omega_0^2LC_p} \end{aligned} \tag{2}$$

where τ denotes the dimensionless time and ω_0 denotes the natural frequency of the corresponding linear mechanical system, l is the thickness of piezoceramic layer as a reference length, α is the dimensionless cubic nonlinearity coefficient, μ is the dimensionless mechanical damping, χ denotes the dimensionless electromechanical coupling, β and γ are two dimensionless time constants. It is noteworthy that the transformations (2) herein ensure the essence of two-way coupling between the mechanical system and the electrical system of NPEHs and hence the consistency of the analysis on energy conversion efficiency performed on the base of the dimensional framework and the dimensionless framework.

Since the ambient base excitation is typically distributed over a broad frequency spectrum, and thus, the ambient excitation is assumed to be a white Gaussian noise $\zeta(\tau)$ with zero mean value and its correlation function $E[\zeta(\tau)\zeta(s)] = 2D\delta(s - \tau)$. Here δ is the Dirac-delta function, and $2D$ is the noise intensity. Under the above rescaling system (1) becomes, after dropping all overbars for convenience

$$X''(\tau) + \mu X'(\tau) + X(\tau) - \chi V(\tau) + \alpha X(\tau)^3 = \zeta(\tau) \tag{3a}$$

$$V''(\tau) + \chi X''(\tau) + \beta V'(\tau) + \gamma V(\tau) = 0 \tag{3b}$$

where the prime represents the differential with respect to τ . According to Itô differential rules [36, 37], the response statistics on the stochastic dynamics of system (3) can be resolved by rewriting the system in the following Itô stochastic form

$$d\mathbf{x}(\tau) = \mathbf{F}_{NL}(\mathbf{x}, \tau)d\tau + \mathbf{G}_{NL}(\mathbf{x}, \tau)dB(\tau) \tag{4}$$

where the state vector $\mathbf{x} = [X \ X' \ V \ V']^T$, $B(\tau)$ represents a Brownian motion, and

$$\mathbf{F}_{NL}(\mathbf{x}, \tau) = \begin{bmatrix} X' \\ -\mu X' - X + \chi V - \alpha X^3 \\ V' \\ \chi(\mu X' + X + \alpha X^3) - \beta V' - (\gamma + \chi^2)V \end{bmatrix}, \tag{5}$$

$$\mathbf{G}_{NL}(\mathbf{x}, \tau) = \begin{bmatrix} 0 \\ \sqrt{2D} \\ 0 \\ -\chi\sqrt{2D} \end{bmatrix}$$

3 Purely inductive circuit

For a purely inductive circuit, the resistance load R is set extremely large to create the scenario when no current flows in the resistive branch. Consequently, the dimensionless parameter β vanishes.

The response of (4) is depending on the evolution of the transition probability density function (TPDF) $P(\mathbf{x}, \tau)$, which, in turn, is determined by the following Fokker–Planck–Kolmogorov (FPK) equation with $\beta = 0$

$$\begin{aligned} \frac{\partial P(\mathbf{x}, \tau)}{\partial \tau} = & -\frac{\partial}{\partial X} [X'P(\mathbf{x}, \tau)] \\ & -\frac{\partial}{\partial X'} [(-\mu X' - X + \chi V - \alpha X^3)P(\mathbf{x}, \tau)] \\ & -\frac{\partial}{\partial V} [V'P(\mathbf{x}, \tau)] + \frac{1}{2} \frac{\partial^2}{\partial X^2} (2DP(\mathbf{x}, \tau)) \\ & + \frac{1}{2} \frac{\partial^2}{\partial V'^2} (2\chi^2 DP(\mathbf{x}, \tau)) \\ & -\frac{\partial}{\partial V'} [(\chi(\mu X' + X + \alpha X^3) - (\gamma + \chi^2)V)P(\mathbf{x}, \tau)] \\ & -\frac{\partial^2}{\partial X' \partial V'} (2\chi DP(\mathbf{x}, \tau)) \end{aligned} \tag{6}$$

with initial condition $P(\infty, \tau) = P(-\infty, \tau) = 0$.

In this section, we focus on attaining the stationary solution of Eq. (6), which means the TPDF is time invariant, i.e., $P(\mathbf{x})$. Therefore, the exact stationary solution of the PDF can be expressed as

$$\begin{aligned} P(X, X', V, V') \\ = C \exp \left\{ -\frac{\mu}{D} \left[\frac{1}{2} X^2 + \frac{1}{2} X'^2 + \frac{\alpha}{4} X^4 + \frac{1}{2} V^2 + \frac{1}{2\gamma} (\chi X' + V')^2 \right] \right\} \end{aligned} \tag{7}$$

where C is a normalization constant which satisfies the following normalization condition

$$\int_{-\infty}^{\infty} \int_{-\infty}^{\infty} \int_{-\infty}^{\infty} \int_{-\infty}^{\infty} P(X, X', V, V') dXdX'dVdV' = 1 \tag{8}$$

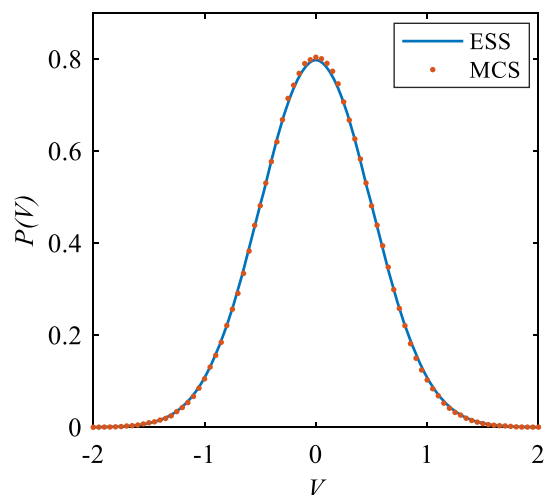


Fig. 2 The exact stationary PDF of voltage. $2D = 0.05$, $\alpha = 1$, $\mu = 0.1$, $\chi = -0.6$, $\gamma = 1$

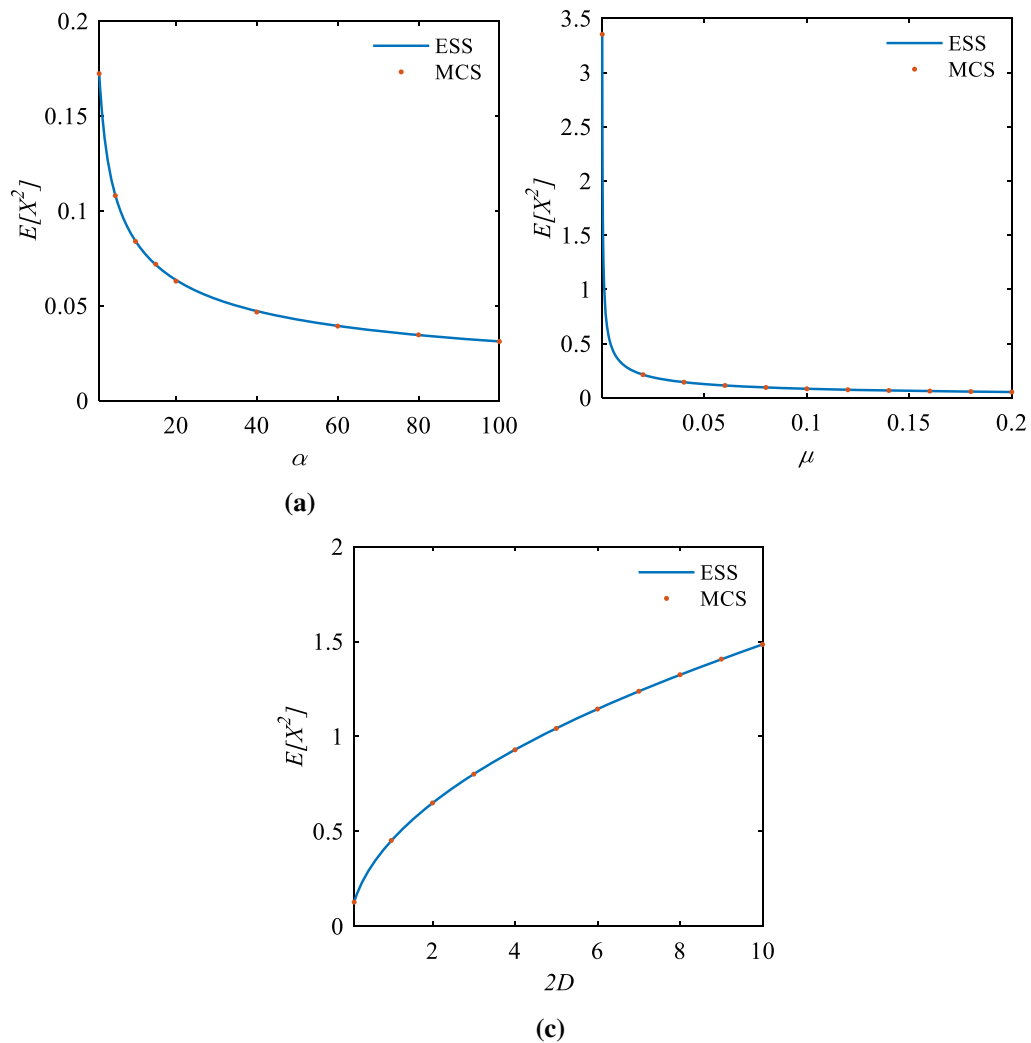


Fig. 3 Variation of mean square displacement with (a) nonlinearity α , (b) mechanical damping μ and (c) noise intensity $2D$

The probability density function (PDF) of output voltage can then be obtained as

$$\begin{aligned}
 P(V) &= \int_{-\infty}^{\infty} \int_{-\infty}^{\infty} \int_{-\infty}^{\infty} P(X, X', V, V') dX dX' dV' \\
 &= \frac{\sqrt{\mu}}{\sqrt{2\pi D}} \exp\left(-\frac{\mu V^2}{2D}\right) \tag{9}
 \end{aligned}$$

Figure 2 demonstrates the comparison between the exact stationary solution (ESS) and Monte Carlo simulations (MCS) of the PDF of the voltage response. It is noteworthy that, due to the existence of exact stationary solution, even if we increase the nonlinearity and the noise intensity of random excitations, the analytical solution and the numerical result still

matches very well, thus, the verified results are omitted. That feature immensely broadens the scope of application of the present analytical solution to the scenario of severe nonlinearity and excitation.

On the basis of the exact stationary PDF, the mean square voltage has the simple expression

$$E[V^2] = \int_{-\infty}^{\infty} V^2 P(V) dV = \frac{D}{\mu} \tag{10a}$$

Similarly, the mean square velocity and mean square displacement are expressed as

$$E[X^2] = \frac{D}{\mu} \tag{10b}$$

$$E[X^2] = \frac{BesselK\left(\frac{3}{4}, \frac{\mu}{8\alpha D}\right) - BesselK\left(\frac{1}{4}, \frac{\mu}{8\alpha D}\right)}{2\alpha BesselK\left(\frac{1}{4}, \frac{\mu}{8\alpha D}\right)} \quad (10c)$$

where $BesselK$ represents the modified Bessel function of second kind. The variations of the mean square displacement with respect to the nonlinearity α , mechanical damping μ and noise intensity $2D$ are, respectively, shown in Fig. 3.

The formula in (10) states that for the purely inductive circuit, the mean square displacement depends only on the nonlinearity, the noise intensity and the mechanical damping, while the mean square voltage is completely independent of the time constant γ , the electromechanical coupling and the nonlinearity, and proportional to the noise intensity but inversely proportional to the mechanical damping. Actually, considering the fact that the mechanical damping in practical engineering is a small but finite value, the mean square voltage can never approach infinite value. Note that, the astonishing result expressed by (10) holds only in the case of PEHs with a resonant circuit under white Gaussian noises and can also be verified by the degenerated exact solution (setting β to be zero) obtained in our recent research on linear PEHs with a resonant circuit [49]. Consequently, both a linear and a nonlinear energy harvester produce the same mean square voltage. In fact, from the perspective of energy balance, as discussed in Sect. 4, for the purely inductive circuit, the input power, D , is completely dissipated by the mechanical damping due to the null output power caused by $\beta = 0$, thus, the simple formula expressed by (10b) is naturally generated. Although the white Gaussian noise is an ideal model to describe to the ambient excitation with broadband property, we could be also inspired by the present result that PEHs may be applied to the ultra-wide-band circumstances without considering the optimized piezo properties and electrical parameters when the purely inductive circuit condition is allowed in the specific applications.

4 Resistive–inductive circuit

For a resistive–inductive circuit, that is $\beta \neq 0$, it is almost impossible to attain an exact stationary PDF of the state variables. Some researchers strove to acquire an approximate solution of the NPEHs with a purely resistive circuit using analytical methods [39–42].

However, as a result of the particularity of the NPEHs with a resonant circuit, the conventional stochastic averaging method based on Hamiltonian mechanics will be invalid. Most important, we would like to further explore analytical solutions available to the strong two-way coupling electromechanical system. Consequently, hereafter, we apply a direct equivalent linearization technique [52] to approximate the response statistics of the NPEHs with a resonant circuit.

4.1 Equivalent linearization technique

The purpose in this section is to estimate the response behavior of the original nonlinear system in terms of a linear system. We first write nonlinear Eq. (3) in a compact form

$$\mathbf{g}(\mathbf{U}'', \mathbf{U}', \mathbf{U}) = \mathbf{f}(\tau) \quad (11)$$

where $\mathbf{U} = [X \ V]^T$, and

$$\mathbf{g} = \begin{bmatrix} X'' + \mu X' + X + \alpha X^3 - \chi V \\ \chi X'' + V'' + \beta V' + \gamma V \end{bmatrix}, \mathbf{f} = \begin{bmatrix} \xi(\tau) \\ 0 \end{bmatrix} \quad (12)$$

Assuming that a stationary solution to nonlinear system (11) exists. Then, we define the following linear equations

$$\mathbf{M}\mathbf{U}'' + \mathbf{C}\mathbf{U}' + \mathbf{K}\mathbf{U} = \mathbf{f}(\tau) \quad (13)$$

to afford an approximate solution to the nonlinear system (11). Here, \mathbf{M} , \mathbf{C} and \mathbf{K} are equivalent matrix on mass, damping and stiffness, respectively, which will be determined later. Next, we define the difference of the two systems, (11) and (13), as the error, which are expressed as

$$\mathbf{e} = \mathbf{g}(\mathbf{U}'', \mathbf{U}', \mathbf{U}) - \mathbf{M}\mathbf{U}'' - \mathbf{C}\mathbf{U}' - \mathbf{K}\mathbf{U} \quad (14)$$

Note that \mathbf{U} in Eq. (14) is the response matrix of system (13). In the purpose of selecting \mathbf{M} , \mathbf{C} and \mathbf{K} effectively, the error \mathbf{e} should be controlled as small as possible. Minimizing the mean square value of \mathbf{e} would be an effective criterion, i.e.,

$$E[\mathbf{e}^T \mathbf{e}] \rightarrow \text{minimum} \quad (15)$$

In fact, the criterion (15) implies the necessary conditions

$$\begin{aligned} \frac{\partial}{\partial m_{ij}} E[\mathbf{e}^T \mathbf{e}] &= 0, \frac{\partial}{\partial c_{ij}} E[\mathbf{e}^T \mathbf{e}] = 0, \frac{\partial}{\partial k_{ij}} E[\mathbf{e}^T \mathbf{e}] \\ &= 0, (i, j = 1, 2) \end{aligned} \tag{16}$$

Substituting (14) into (16) and implementing the partial differentiations leads to the following equations

$$E[\mathbf{z}\mathbf{z}^T][\mathbf{M} \ \mathbf{C} \ \mathbf{K}]^T = E[\mathbf{z}\mathbf{g}^T] \tag{17}$$

where

$$\mathbf{z}^T = [(\mathbf{U}'')^T \ (\mathbf{U}')^T \ \mathbf{U}^T] \tag{18}$$

Note that, since the excitation vector in (13) is Gaussian with zero mean, so as the vector \mathbf{z} . Hence, the expression $E[\mathbf{z}\mathbf{g}^T]$ can be written by

$$E[\mathbf{z}\mathbf{g}^T] = E[\mathbf{z}\mathbf{z}^T]E[\nabla\mathbf{g}^T] \tag{19}$$

where

$$\nabla^T = \left[\frac{\partial}{\partial X} \ \frac{\partial}{\partial V} \right] \tag{20}$$

Substituting (19) into (17) yields

$$E[\mathbf{z}\mathbf{z}^T][\mathbf{M} \ \mathbf{C} \ \mathbf{K}]^T = E[\mathbf{z}\mathbf{z}^T]E[\nabla\mathbf{g}^T] \tag{21}$$

Recall that \mathbf{z} is Gaussian with zero mean, then the covariance matrix $E[\mathbf{z}\mathbf{z}^T]$ of \mathbf{z} will be either positive semidefinite or positive definite. Actually, no matter the covariance matrix $E[\mathbf{z}\mathbf{z}^T]$ is positive semidefinite or positive definite, the solution of (21) will always correspond to a minimum.

Finally, the solution of (21) can be obtained

$$[\mathbf{M} \ \mathbf{C} \ \mathbf{K}]^T = E[\nabla\mathbf{g}^T] \tag{22}$$

Utilizing (18), then each term of \mathbf{M} , \mathbf{C} and \mathbf{K} matrices are expressed as

$$\begin{aligned} m_{11} &= E\left[\frac{\partial g_1}{\partial X''}\right] = 1, m_{12} = E\left[\frac{\partial g_1}{\partial V''}\right] = 0, m_{21} = E\left[\frac{\partial g_2}{\partial X''}\right] = \chi \\ m_{22} &= E\left[\frac{\partial g_2}{\partial V''}\right] = 1, c_{11} = E\left[\frac{\partial g_1}{\partial X'}\right] = \mu, c_{12} = E\left[\frac{\partial g_1}{\partial V'}\right] = 0 \\ c_{21} &= E\left[\frac{\partial g_2}{\partial X'}\right] = 0, c_{22} = E\left[\frac{\partial g_2}{\partial V'}\right] = \beta, k_{11} = E\left[\frac{\partial g_1}{\partial X}\right] \\ &= 1 + 3\alpha E[X^2] \\ k_{12} &= E\left[\frac{\partial g_1}{\partial V}\right] = -\chi, k_{21} = E\left[\frac{\partial g_2}{\partial X}\right] = 0, k_{22} = E\left[\frac{\partial g_2}{\partial V}\right] = \gamma \end{aligned} \tag{23}$$

Thus, the exact expression of the equivalent matrices in linear system (13) are attained. Observing (23), evidently, the linear system (13)'s equivalent matrices, in turn, rely on the response statistics. It is noteworthy that if higher nonlinearities are contained in the original system (3), higher-order statistics will arise in the coefficients and can be determined by repeated application of the identity relation (19).

Further, the second-order moments of system (13) can be obtained by any of the existing analytical methods. Herein, the moment equation method [36, 37] is employed to attain the closed form of the second-order moments. To this end, the equivalent linearization system (13) can be further expressed in the Itô stochastic differential equation

$$d\mathbf{x}(\tau) = \mathbf{F}(\mathbf{x}, \tau)d\tau + \mathbf{G}(\mathbf{x}, \tau)dB(\tau) \tag{24}$$

where

$$\begin{aligned} \mathbf{F}(\mathbf{x}, \tau) &= \begin{bmatrix} X' \\ -\mu X' - k_{11}X + \chi V \\ V' \\ \chi\mu X' + \chi k_{11}X - \beta V' - (\gamma + \chi^2)V \end{bmatrix}, \\ \mathbf{G}(\mathbf{x}, \tau) &= \begin{bmatrix} 0 \\ \sqrt{2D} \\ 0 \\ -\chi\sqrt{2D} \end{bmatrix} \end{aligned} \tag{25}$$

Consider a polynomial function $M = X^{n_1} X^{n_2} V^{n_3} V^{n_4}$, according to Itô's lemma, we have

$$\begin{aligned} dM &= \frac{\partial M}{\partial X} dX + \frac{\partial M}{\partial X'} dX' + \frac{\partial M}{\partial V} dV + \frac{\partial M}{\partial V'} dV' \\ &+ \frac{1}{2} \frac{\partial^2 M}{\partial X'^2} (dX')^2 + \frac{1}{2} \frac{\partial^2 M}{\partial V'^2} (dV')^2 \\ &+ \frac{\partial^2 M}{\partial X' \partial V'} (dX')(dV') \end{aligned} \tag{26}$$

Recall that in the Itô sense, the state variables in \mathbf{x} are independent of $dB(\tau)$. Taking the mathematical expectation on both sides of Eq. (26) and keeping the terms up to the order $d\tau$ yields

$$\begin{aligned}
 \frac{dE[M]}{d\tau} &= \frac{dm_{n_1, n_2, n_3, n_4}}{d\tau} \\
 &= n_1 m_{n_1-1, n_2+1, n_3, n_4} - (\mu n_2 + \beta n_4) m_{n_1, n_2, n_3, n_4} \\
 &\quad - n_2 k_{11} m_{n_1+1, n_2-1, n_3, n_4} + \chi n_2 m_{n_1, n_2-1, n_3+1, n_4} \\
 &\quad + \chi \mu n_4 m_{n_1, n_2+1, n_3, n_4-1} \\
 &\quad + \chi n_4 k_{11} m_{n_1+1, n_2, n_3, n_4-1} \\
 &\quad + n_4 \chi^2 D(n_4 - 1) m_{n_1, n_2, n_3, n_4-2} \\
 &\quad + n_3 m_{n_1, n_2, n_3-1, n_4+1} \\
 &\quad + n_2 D(n_2 - 1) m_{n_1, n_2-2, n_3, n_4} \\
 &\quad - (\gamma + \chi^2) n_4 m_{n_1, n_2, n_3+1, n_4-1} \\
 &\quad - 2\chi n_2 n_4 D m_{n_1, n_2-1, n_3, n_4-1}
 \end{aligned} \tag{27}$$

Selecting the pairs of the power indices (n_1, n_2, n_3, n_4) to satisfy the relationship $n_1 + n_2 + n_3 + n_4 = 2$, the moment differential equations can be derived as

$$\begin{aligned}
 \frac{d}{d\tau} E[X^2] &= 2E[XX'], \frac{d}{d\tau} E[V^2] = 2E[VV'] \\
 \frac{d}{d\tau} E[XX'] &= E[X'^2] - \mu E[XX'] - k_{11} E[X^2] + \chi E[XV] \\
 \frac{d}{d\tau} E[XV] &= E[X'V] + E[XV'] \\
 \frac{d}{d\tau} E[XV'] &= E[X'V'] + \chi \mu E[XX'] - \beta E[XV'] \\
 &\quad + \chi k_{11} E[X^2] - (\gamma + \chi^2) E[XV] \\
 \frac{d}{d\tau} E[X'^2] &= 2D - 2\mu E[X'^2] - 2k_{11} E[XX'] + 2\chi E[X'V] \\
 \frac{d}{d\tau} E[X'V] &= E[X'V'] - \mu E[X'V] - k_{11} E[XV] + \chi E[V^2] \\
 \frac{d}{d\tau} E[X'V'] &= \chi E[VV'] + \chi \mu E[X'^2] + \chi k_{11} E[XX'] \\
 &\quad - k_{11} E[XV'] - \mu E[X'V'] - \beta E[X'V'] \\
 &\quad - (\gamma + \chi^2) E[X'V] - 2\chi D \\
 \frac{d}{d\tau} E[V'^2] &= 2\chi \mu E[X'V'] + 2\chi k_{11} E[XV'] \\
 &\quad - 2\beta E[V'^2] - 2(\gamma + \chi^2) E[VV'] + 2\chi^2 D \\
 \frac{d}{d\tau} E[VV'] &= E[V'^2] + \chi \mu E[X'V] + \chi k_{11} E[XV] \\
 &\quad - \beta E[VV'] - (\gamma + \chi^2) E[V^2]
 \end{aligned} \tag{28}$$

By setting the time derivatives of the moments to zero in Eq. (28), we obtain the steady-state solutions of above moment equations as follows

$$E[V^2] = \frac{\chi^2 D(\beta k_{11} + \gamma \mu)}{\beta \mu k_{11}^2 + [\beta^2 \mu + \beta(\mu^2 + \chi^2) + \chi^2 \mu - 2]\beta k_{11} + \beta \mu \gamma(\chi^2 + \mu^2 + \gamma + \beta \mu) + \chi^2 \gamma \mu^2} \tag{29a}$$

$$E[X^2] = \frac{D[\beta k_{11}^2 + (\beta^2 + \beta \mu + \chi^2 - 2\gamma)\beta k_{11} + \beta \gamma(\mu^2 + \gamma + \beta \mu) + \chi^2 \gamma \mu]}{\beta \mu k_{11}^2 + [\beta^2 \mu + \beta(\mu^2 + \chi^2) + \chi^2 \mu - 2\gamma \mu]\beta k_{11} + \beta \mu \gamma(\chi^2 + \mu^2 + \gamma + \beta \mu) + \chi^2 \gamma \mu^2} \tag{29b}$$

$$E[X^2] = \frac{D[\beta k_{11}^2 + (\beta^2 + \beta \mu - 2\gamma)\beta k_{11} + \beta \gamma(\chi^2 + \mu^2 + \gamma + \beta \mu) + \chi^2 \gamma \mu]}{\beta \mu k_{11}^2 + [\beta^2 \mu + \beta(\mu^2 + \chi^2) + \chi^2 \mu - 2\gamma \mu]\beta k_{11} + \beta \mu \gamma(\chi^2 + \mu^2 + \gamma + \beta \mu) + \chi^2 \gamma \mu^2} \tag{29c}$$

Substituting the expression of $E[X^2]$ into the relationship $k_{11} = 1 + 3\alpha E[X^2]$, and taking a cyclic procedure on it, the convergence value of k_{11} and $E[X^2]$ can be determined. Meanwhile, the averaged output power has the simple form

$$E[P_{out}] = \beta E[V^2] \tag{30}$$

4.2 Efficiency calculation

Efficiency, the ratio of the net electrical output power to the net mechanical input power, is an important performance metric. Based on the efficiency analysis of directly excited [50] and parametrically excited [53] PEHs, the input mechanical energy, actually, is influenced by the phase difference between the dynamical response and the deterministic excitation. Our recent study has found that by taking advantage of the energy balance equation of electromechanical coupling system, mathematical expressions on the input mechanical energy and the output electrical energy can be generated naturally and rational efficiency analysis can be achieved [49, 53]. In this subsection, the energy conversion efficiency of the NPEHs with a resonant circuit under white Gaussian noises is examined via the mean power balance equation.

The Itô stochastic equation describing the NPEHs with a resonant circuit has an invariant H expressed as follows

$$\begin{aligned}
 H &= \frac{1}{2}(1 + \chi^2)X^2 + \frac{1}{2}X'^2 + \frac{1}{4}\alpha X^4 + \frac{1}{2}(\chi X + V)^2 \\
 &\quad + \frac{1}{2\gamma}(\chi X' + V')^2 - \chi X(\chi X + V)
 \end{aligned} \tag{31}$$

The differential of this invariant in the Itô sense becomes

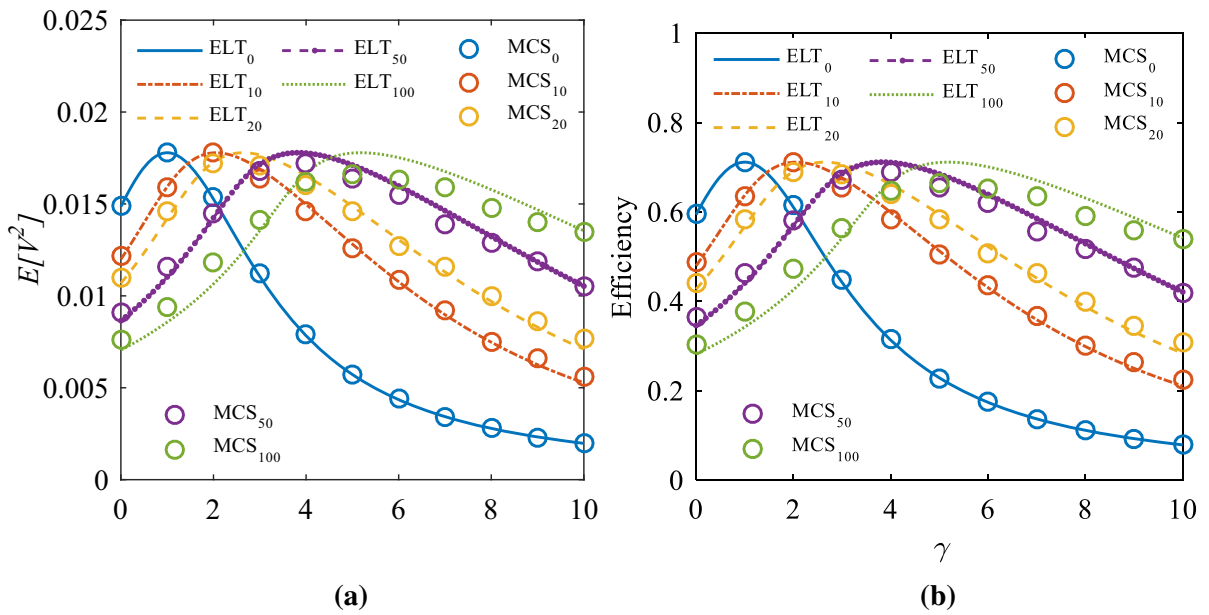


Fig. 4 Variation of (a) mean square voltage and (b) efficiency with time constant γ . $\beta = 1, \mu = 0.1, \chi = -0.6, 2D = 0.05, \alpha = 0$ (ELT₀ and MCS₀), $\alpha = 10$ (ELT₁₀ and MCS₁₀), $\alpha = 20$ (ELT₂₀ and MCS₂₀), $\alpha = 50$ (ELT₅₀ and MCS₅₀), $\alpha = 100$ (ELT₁₀₀ and MCS₁₀₀)

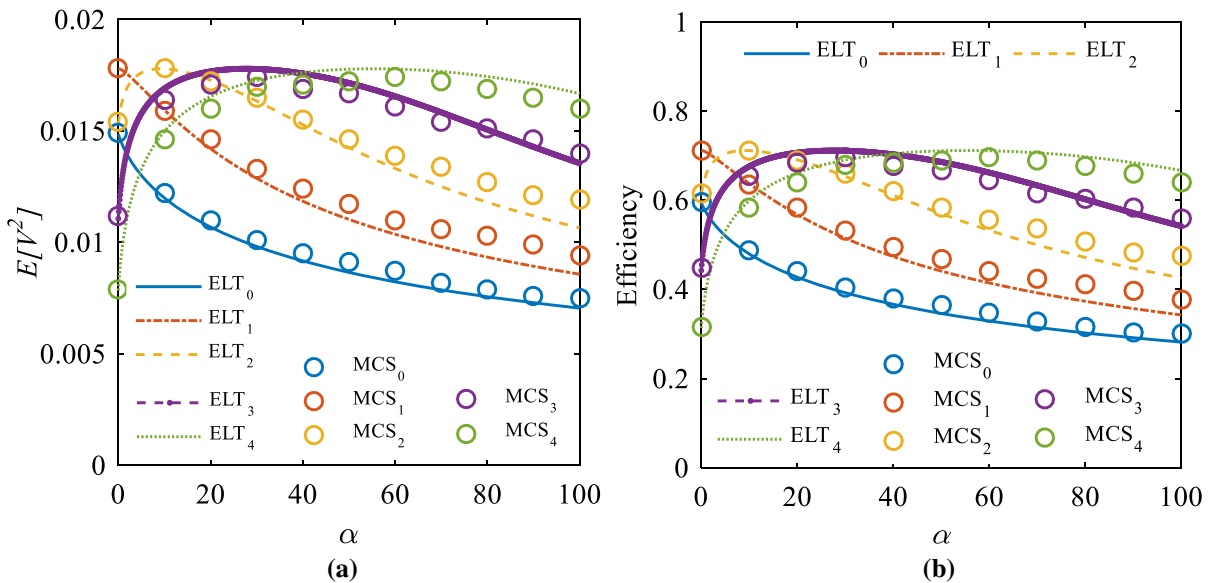


Fig. 5 Variation of (a) mean square voltage and (b) efficiency with nonlinearity α . $\beta = 1, \mu = 0.1, \chi = -0.6, 2D = 0.05, \gamma = 0$ (ELT₀ and MCS₀), $\gamma = 1$ (ELT₁ and MCS₁), $\gamma = 2$ (ELT₂ and MCS₂), $\gamma = 3$ (ELT₃ and MCS₃), $\gamma = 4$ (ELT₄ and MCS₄)

$$dH = \frac{\partial H}{\partial X} dX + \frac{\partial H}{\partial X'} dX' + \frac{\partial H}{\partial V} dV + \frac{\partial H}{\partial V'} dV' + \frac{1}{2} \frac{\partial^2 H}{\partial X^2} (dX')^2 + \frac{1}{2} \frac{\partial^2 H}{\partial V^2} (dV')^2 + \frac{\partial^2 H}{\partial X' \partial V'} (dX')(dV') \tag{32}$$

Taking the mathematical expectation on both sides of Eq. (32) and keeping the terms up to the order $d\tau$ yields the mean power balance equation

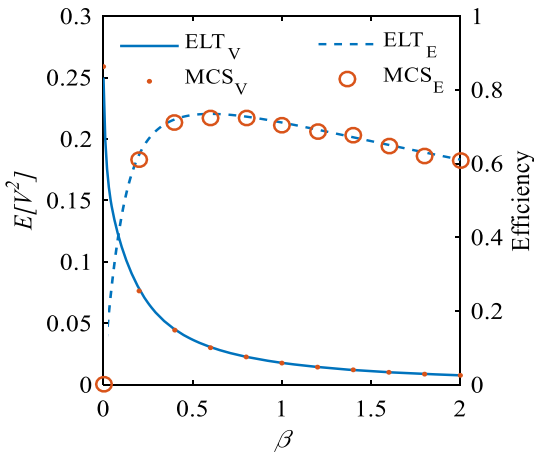


Fig. 6 Variation of mean square voltage (ELT_V and MCS_V) and efficiency (ELT_E and MCS_E) with time constant β . $\mu = 0.1$, $\chi = -0.6$, $2D = 0.05$, $\alpha = 10$, $\gamma = 2$

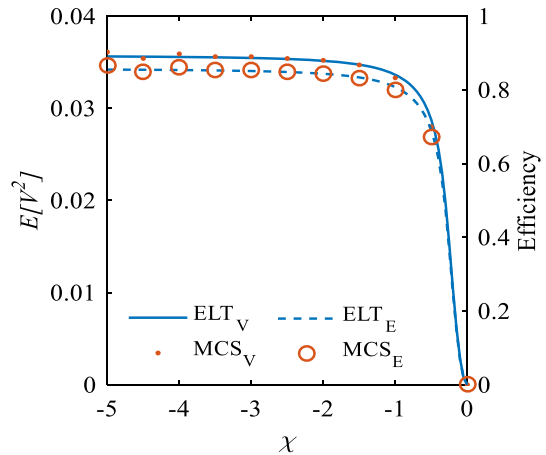


Fig. 8 Variation of mean square voltage (ELT_V and MCS_V) and efficiency (ELT_E and MCS_E) with electromechanical coupling χ . $\beta = 0.6$, $\mu = 0.1$, $2D = 0.05$, $\alpha = 10$, $\gamma = 2$

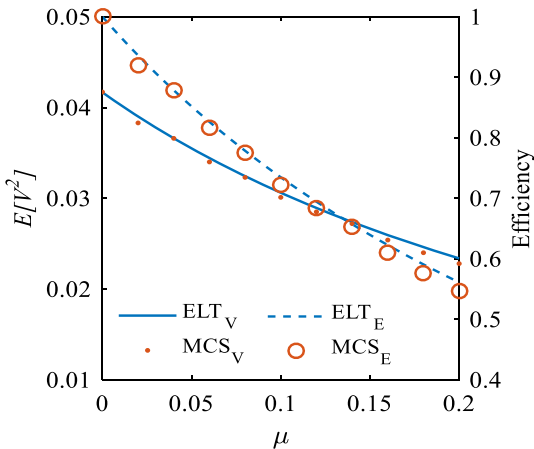


Fig. 7 Variation of mean square voltage (ELT_V and MCS_V) and efficiency (ELT_E and MCS_E) with mechanical damping μ . $\beta = 0.6$, $\chi = -0.6$, $2D = 0.05$, $\alpha = 10$, $\gamma = 2$

$$\frac{dE[H]}{d\tau} = D - \mu E[X^2] - \frac{\chi\beta}{\gamma} E[X'V'] - \frac{\beta}{\gamma} E[V^2] \tag{33}$$

where D is the net input power supplied by ambient noise, denoted by $E[P_{in}]$, $\mu E[X^2]$ represents the power dissipated by the mechanical damping. Revisiting Eq. (28), in the steady state, the net output power $\beta E[V^2]$, dissipated by the load resistance and denoted by $E[P_{out}]$, is equal to $\chi\beta E[X'V']/\gamma$ plus $\beta E[V^2]/\gamma$. Therefore, the efficiency of the NPEHs under white Gaussian noises can be given in the following simple form

$$\eta = \frac{E[P_{out}]}{E[P_{in}]} = \frac{\beta E[V^2]}{D} \tag{34}$$

Evidently, the averaged power input is just in proportion with respect to the noise intensity. We note that the variation of the efficiency with respect to the dimensionless system parameters is actually the same as that of the averaged output power, due to the fact that the averaged input power is a constant for the NPEHs excited by white Gaussian noises.

Equation (29), Eq. (30), and Eq. (34) indicate that performance metrics are associated with all the dimensionless parameters involving the mechanical system and the electrical system. Therefore, in order to achieve a high performance, we need take comprehensive consideration of all factors, including ambient excitation, material, structure and circuit element.

5 Results and discussion

In this section, mean square voltage and energy conversion efficiency (averaged power output) as typical performance metrics obtained in Sect. 4 by means of equivalent linearization technique (ELT) are now examined. In addition, Monte Carlo simulations (MCS) of the original system (3) are implemented to validate the theoretical results, as expressed by circles and dots in Figs. 4, 5, 6, 7, 8, 9.

Figure 4 shows that the variation of the mean square voltage and the efficiency (averaged power

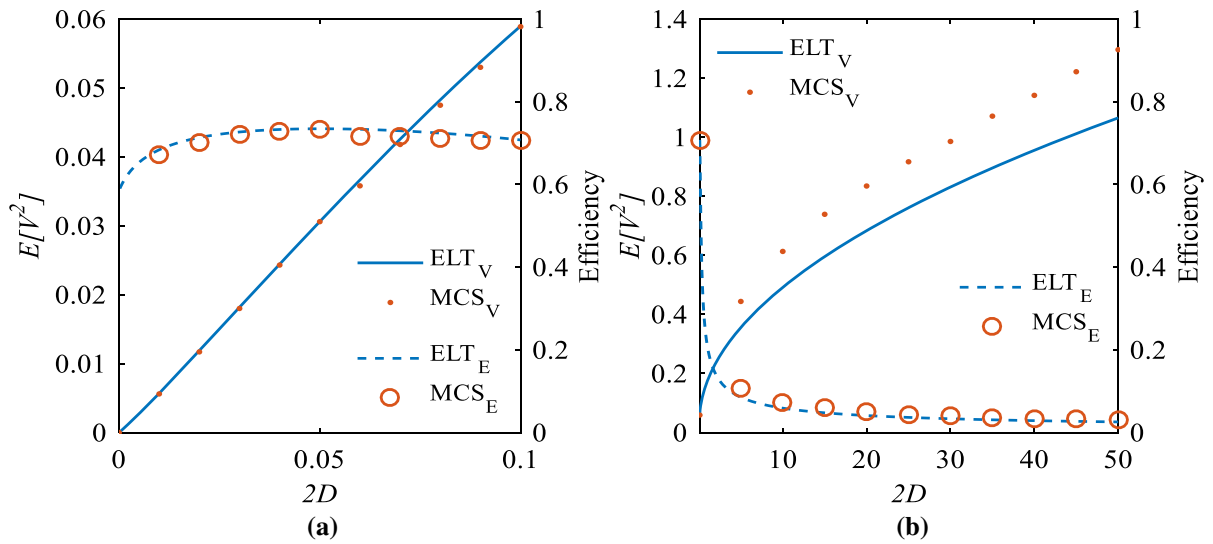


Fig. 9 Variation of mean square voltage (ELT_V and MCS_V) and efficiency (ELT_E and MCS_E) with noise intensity $2D$ (a) 0–0.1, (b) 0.1–50. $\beta = 0.6$, $\mu = 0.1$, $\chi = -0.6$, $\alpha = 10$, $\gamma = 2$

output) with respect to the time constant γ for five different nonlinearities. It is evident that γ has quite an influence on the performance metrics of the NPEHs with a resonant circuit. As γ is increased, the mean square voltage and efficiency (averaged power output) peak at the same certain optimal value corresponding to a nonlinearity level. For the linear scenario ($\alpha = 0$), the maximum performance metrics with a resonant circuit arises when the intrinsic frequency of the electrical system is equal to that of the mechanical system, which can be regarded as a perfect matching condition between two oscillatory systems. As the nonlinearity α is increased, the optimal γ shifts toward the larger value but the maximum value of performance metrics almost keeps a constant, just like the linear scenario. This intriguing phenomenon can be explained that the increased nonlinearity increases the nonlinear frequency of the mechanical system and thus drives the electrical system to shift its linear resonant frequency toward the larger value to maximize the energy transport from the mechanical system to the electrical system. Note that the results obtained by ELT have a perfect match with those of MCS when the linear scenario is considered and the error is slightly amplified when the nonlinearity increases.

On the other hand, Fig. 5 depicts the variation of performance metrics with respect to the nonlinearity α for five different time constant γ . It is clearly seen that the variation law of performance metrics contains two

different features depending on γ . Specifically, when γ is smaller than the optimal value of the linear scenario, as α is increased, the performance metrics decreases monotonically. However, when γ is larger than the optimal value of the linear scenario, as α is increased, the performance metrics peak at the different optimal α value, but share the same maximum value as that of the linear scenario ($\alpha = 0$, $\gamma = 1$). That means that, for real applications, it is important even for PEHs which do not intentionally incorporate nonlinearities. To be specific, since most mechanical systems of PEHs exhibit some inherent stiffness nonlinearities with hardening cubic type, once its nonlinear coefficients are determined by analytical or experimental method, then, the optimal operating time constant γ of the electrical system should be chosen such that the appropriate combination of nonlinearity and time constant can help maximize the performance metrics. Such coupling effect between nonlinearity and time constant as a unique characteristic, in contrast to the NPEHs with a purely resistive circuit [39], actually, provide an opportunity to extend the scope of applications of the NPEHs with a resonant circuit.

Picking up a set of optimal parameters ($\alpha = 10$, $\gamma = 2$), the influences of the time constant β , mechanical damping μ , electromechanical coupling χ , and also ambient noise intensity $2D$ on performance metrics are shown in Figs. 6, 7, 8, 9, respectively. For the purely inductive circuit scenario ($\beta = 0$), as we

expect, the mean square voltage reaches the maximum value. As β is increased gradually from zero, the mean square voltage decreases dramatically, and then tends to a small value. Nevertheless, the efficiency increases rapidly until reaching the maximum value at $\beta = 0.6$ and then decrease slowly, see Fig. 6. Figure 7 demonstrates that the performance metrics monotonically decrease as the mechanical damping μ is increased. It is noteworthy that, if unnecessary loss in the electrical system, such as dielectric loss and current leakage, is ignored, mechanical damping as the only irreversible dissipation factor, will adversely influence the performance, and the overall energy conversion efficiency delivered by the ambient noise to the net electrical energy tends to 100% as μ is infinitely reduced [49, 50, 53]. As shown in Fig. 8, the stronger the electromechanical coupling is, the higher performance the NPEHs occupy. In fact, performance of the PEHs with a resonant circuit can converge toward the maximum faster than the PEHs with purely resistive circuit as the coupling level is enhanced [49]. Consequently, there is no need to infinitely improve the electromechanical conversion factor of piezoelectric materials. Figure 9 reveals that the mean square voltage monotonically increases as the noise intensity is increased, while the efficiency peak at the optimal value $2D = 0.05$ and then drop dramatically as the noise intensity is increased further, that is, the variation law of the mean square voltage with respect to the noise intensity does not coincide with that of the efficiency. Moreover, the result of the NPEHs with a resonant circuit depicted by Fig. 9 is different with that of the linear scenario (refer to [49]). In the linear scenario, mean square voltage and averaged power output proportionally increase with the noise intensity, while efficiency always remains constant. The features in this nonlinear scenario can actually be explained that increased noise intensity essentially alters the values of optimal parameters combination involving the nonlinearity α and time constant γ . It is imaginable that dynamic tuning the values of optimal parameters combination in this nonlinear scenario will lead the performance to degenerate to the linear scenario. In addition, it is inspiring to see that, although the error between ELM and MCS is gradually amplified with the noise intensity, the error will always be controlled within 20% even if the NPEHs are excited by severe random noises.

6 Conclusion

In this investigation, we theoretically and numerically study the performance of a nonlinear piezoelectric energy harvester with a resonant circuit operating under broadband random excitations. New dimensionless transformations which can seize the essential property of two-way electromechanical coupling are employed to attain a dimensionless dynamical system. Two scenarios, namely the purely inductive circuit and the resistive–inductive circuit, are considered. The exact stationary solution and the direct equivalent linearization solution available to the strong two-way coupling electromechanical system are, respectively, obtained for such two scenarios. The variation law of the performance metrics with dimensionless parameters is revealed and the optimal parameter values for which the performance is maximized are discussed. Monte Carlo numerical simulations are also implemented to validate the theoretical predictions.

For the purely inductive circuit scenario, the exact stationary solution of probability density function of the voltage output and the closed-form expressions of the mean square voltage, velocity and displacement are obtained. It is clearly seen that, in order to maximize the mean square value of the voltage output, the mechanical damping should be minimized and the noise intensity should be as large as possible.

For the resistive–inductive circuit scenario, the approximate solution of mean square voltage and averaged power output are derived by the moment method of random process theory, based on the equivalent linear electromechanical system. Energy conversion efficiency, the ratio of the electrical power net output to the mechanical power net input, is also analyzed by means of energy balance equation. Results indicate that the maximum performance metrics occur when the intrinsic frequency of the electrical circuit system matches the nonlinear frequency of the mechanical system. Selecting appropriate parameters combinations involving nonlinearity α and time constant γ can design outperformed NPEHs. The time constant β should also be optimized to attain the maximum averaged power output and efficiency. There seems to be a limit performance of the harvesters as the electromechanical coupling continuously enhances, that suggests researchers to reasonably evaluate the cost-effectiveness ratio of piezoelectric materials. For the general passive

NPEHs with fixed system parameters, from the perspective of improving the efficiency, an optimal noise intensity exists in the range of weak excitation level. This inspires us to evaluate the harvester's performance using a set of figures of merit, such as mean square voltage, averaged power output, efficiency, etc. It is noteworthy that the direct equivalent linearization method produces rational results even for the severe noise and nonlinearity. That feature immensely broadens the scope of possible application of the direct equivalent linearization method.

The analytical expressions derived in this paper are useful in quantifying the performance of the NPEHs with a resonant circuit when the mechanical system is excited by white Gaussian noises. The importance of the present study is to provide a simple but effective analysis strategy by applying the method of nonlinear stochastic dynamics combined with the energy balance equation to design vibration-based energy harvesters in the more practical setting.

Acknowledgements The authors gratefully acknowledge that the financial support from the National Natural Science Foundation of China (11802266, 11802016, 11432012) and the China Postdoctoral Science Foundation (2018M631349).

Compliance with ethical standards

Conflict of interest The authors declare that they have no conflict of interest.

References

- Baerta, K., Gyselinckxa, B., Torfsa, T., Leonova, V., Yazicioglu, F., Brebelsa, S., Donnaya, S., Vanfleteren, J., Beyna, E., Van Hoof, C.: Technologies for highly miniaturized autonomous sensor networks. *Microelectron. J.* **37**, 1563–1568 (2006)
- Bracke, W., Merken, P., Puers, R., Van Hoof, C.: Generic architectures and design methods for autonomous sensors. *Sens. Actuators, A* **135**, 881–888 (2007)
- Khadem, S.E., Shahgholi, M., Hosseini, S.A.A.: Two-mode combination resonances of an in-extensional rotating shaft with large amplitude. *Nonlinear Dyn.* **65**, 217–233 (2011)
- Yabuno, H., Kashimura, T., Inoue, T., Ishida, Y.: Nonlinear normal modes and primary resonance of horizontally supported Jeffcott rotor. *Nonlinear Dyn.* **66**, 377–387 (2011)
- Chávez, J.P., Wiercigroch, M.: Bifurcation analysis of periodic orbits of a non-smooth Jeffcott rotor model. *Commun. Nonlinear Sci. Numer. Simul.* **18**, 2571–2580 (2013)
- Ghayesh, M.H., Farokhi, H., Alici, G.: Size-dependent performance of microgyroscopes. *Int. J. Eng. Sci.* **100**, 99–111 (2016)
- Yu, T.J., Zhou, S., Yang, X.D., Zhang, W.: Multi-pulse chaotic dynamics of an unbalanced Jeffcott rotor with gravity effect. *Nonlinear Dyn.* **87**, 647–664 (2017)
- Païdoussis, M.P.: *Fluid-Structure Interactions: Slender Structures and Axial Flow*. Academic Press, San Diego (1998)
- Panda, L.N., Kar, R.C.: Nonlinear dynamics of a pipe conveying pulsating fluid with parametric and internal resonances. *Nonlinear Dyn.* **49**, 9–30 (2007)
- Ghayesh, M.H., Païdoussis, M.P., Amabili, M.: Nonlinear dynamics of cantilevered extensible pipes conveying fluid. *J. Sound Vib.* **332**, 6405–6418 (2013)
- Chen, L.Q., Zhang, Y.L., Zhang, G.C., Ding, H.: Evolution of the double-jumping in pipes conveying fluid flowing at the supercritical speed. *Int. J. Non-Linear Mech.* **58**, 11–21 (2014)
- Mao, X.Y., Ding, H., Chen, L.Q.: Steady-state response of a fluid-conveying pipe with 3:1 internal resonance in supercritical regime. *Nonlinear Dyn.* **86**, 795–809 (2016)
- Zhang, L.W., Song, Z.G., Liew, K.M.: Computation of aerothermoelastic properties and active flutter control of CNT reinforced functionally graded composite panels in supersonic airflow. *Comput. Method Appl. Mech. Eng.* **300**, 427–441 (2016)
- Yu, T.J., Zhou, S., Yang, X.D., Zhang, W.: Homoclinic orbits and chaos of a supercritical composite panel with free-layer damping treatment in subsonic flow. *Compos. Struct.* **159**, 288–298 (2017)
- Yu, T.J., Zhou, S., Yang, X.D., Zhang, W.: Global dynamics of composite panels with free-layer damping treatment in subsonic flow. *Compos. Struct.* **168**, 247–258 (2017)
- Zhou, S.X., Wang, J.L.: Dual serial vortex-induced energy harvesting system for enhanced energy harvesting. *AIP Adv.* **8**, 075221 (2018)
- Roccia, B.A., Verstraete, M.L., Ceballos, L.R., Balachandran, B., Preidikman, S.: Computational study of aerodynamically coupled piezoelectric harvesters. *J. Intel. Mat. Syst. Str.* **31**, 1578–1593 (2020)
- Wang, J.L., Gu, S.H., Zhang, C.Y., Hu, G.B., Chen, G., Yang, K., Li, H., Lai, Y.Y., Litak, G., Yurchenko, D.: Hybrid wind energy scavenging by coupling vortex-induced vibrations and galloping. *Energy Convers. Manag.* **213**, 112835 (2020)
- Yang, Z.J., Huang, R., Liu, H.J., Zhao, Y.H., Hu, H.Y.: An improved nonlinear reduced-order modeling for transonic aeroelastic systems. *J. Fluid Struct.* **94**, 102926 (2020)
- Zurbuchen, A., Pfenniger, A., Stahel, A., Stoeck, C.T., Vandenberghe, S., Koch, V.M., Vogel, R.: Energy harvesting from the beating heart by a mass imbalance oscillation generator. *Ann. Biomed. Eng.* **41**, 131–141 (2013)
- Pfenniger, A., Wichramarathna, L.N., Vogel, R., Koch, V.M.: Design and realization of an energy harvester using pulsating arterial pressure. *Med. Eng. Phys.* **35**, 1256–1265 (2013)
- Yang, Z.B., Zhou, S.X., Zu, J., Inman, D.: High-performance piezoelectric energy harvesters and their applications. *Joule* **2**, 624–697 (2018)

23. Ali, F., Raza, W., Li, X.L., Gul, H., Kim, K.H.: Piezoelectric energy harvesters for biomedical applications. *Nano Energy* **57**, 879–902 (2019)
24. Daqaq, M.F., Masana, R., Erturk, A., Quinn, D.D.: On the role of nonlinearities in vibratory energy harvesting: a critical review and discussion. *Appl. Mech. Rev.* **66**, 040801 (2014)
25. Tran, N., Ghayesh, M.H., Arjomandi, M.: Ambient vibration energy harvesters: a review on nonlinear techniques for performance enhancement. *Int. J. Eng. Sci.* **127**, 162–185 (2018)
26. Hu, Y., Xue, H., Yang, J., Jiang, Q.: Nonlinear behavior of a piezoelectric power harvester near resonance. *IEEE Trans. Ultrason. Ferroelectr. Freq. Control* **53**, 1387–1391 (2006)
27. Beeby, S.P., Torah, R.N., Tudor, M.J., Glynne-Jones, P., O'Donnell, T., Saha, C.R., Roy, S.: A micro electromagnetic generator for vibration energy harvesting. *J. Micromech. Microeng.* **17**, 1257–1265 (2007)
28. Mann, B.P., Sims, N.D.: Energy harvesting from the nonlinear oscillations of magnetic levitation. *J. Sound Vib.* **319**, 515–530 (2008)
29. Ramlan, R., Brennan, M.J., Mace, B.R., Kovacic, I.: Potential benefits of a non-linear stiffness in an energy harvesting device. *Nonlinear Dyn.* **59**, 545–558 (2010)
30. Hu, G.B., Tang, L.H., Das, R., Marzocca, P.: A two-degree-of-freedom piezoelectric energy harvester with stoppers for achieving enhanced performance. *Int. J. Mech. Sci.* **149**, 500–507 (2018)
31. Zhou, S.X., Zuo, L.: Nonlinear dynamic analysis of asymmetric tristable energy harvesters for enhanced energy harvesting. *Commun. Nonlinear Sci. Numer. Simul.* **61**, 271–284 (2018)
32. Lu, Z.Q., Chen, J., Ding, H., Chen, L.Q.: Two-span piezoelectric beam energy harvesting. *Int. J. Mech. Sci.* **175**, 105532 (2020)
33. Quinn, D.D., Triplett, A.L., Bergman, L.A., Vakakis, A.F.: Comparing linear and essentially nonlinear vibration-based energy harvesting. *ASME J. Vib. Acoust.* **133**, 011001 (2011)
34. Sebal, G., Kuwano, H., Guyomar, D., Ducharme, B.: Simulation of a Duffing oscillator for broadband piezoelectric energy harvesting. *Smart Mater. Struct.* **20**, 075022 (2011)
35. Papoulis, A., Pillai, S.U.: *Probability, Random Variables and Stochastic Processes*, 4th edn. McGraw-Hill, Boston (2002)
36. Sun, J.Q.: *Stochastic Dynamics and Control*. Elsevier, Oxford (2006)
37. Cai, G.Q., Zhu, W.Q.: *Elements of Stochastic Dynamics*. World Scientific Publishing, Singapore (2016)
38. Daqaq, M.F.: Response of uni-modal duffing-type harvesters to random forced excitations. *J. Sound Vib.* **329**, 3621–3631 (2010)
39. Daqaq, M.F.: On intentional introduction of stiffness nonlinearities for energy harvesting under white Gaussian excitations. *Nonlinear Dyn.* **69**, 1063–1079 (2012)
40. Xu, M., Jin, X.L., Wang, Y., Huang, Z.L.: Stochastic averaging for nonlinear vibration energy harvesting system. *Nonlinear Dyn.* **78**, 1451–1459 (2014)
41. Liu, D., Xu, Y., Li, J.L.: Probabilistic response analysis of nonlinear vibration energy harvesting system driven by Gaussian colored noise. *Chaos Soliton. Fract.* **104**, 806–812 (2017)
42. Zhang, Y.X., Jin, Y.F., Xu, P.F.: Dynamics of a coupled nonlinear energy harvester under colored noise and periodic excitations. *Int. J. Mech. Sci.* **172**, 105418 (2020)
43. Gammaitoni, L., Neri, I., Vocca, H.: Nonlinear oscillators for vibration energy harvesting. *Appl. Phys. Lett.* **94**, 164102 (2009)
44. McInnes, C., Gorman, D., Cartmell, M.: Enhanced vibrational energy harvesting using nonlinear stochastic resonance. *J. Sound Vib.* **318**, 655–662 (2008)
45. Masana, R., Daqaq, M.F.: Relative performance of a vibratory energy harvester in mono- and bi-stable potentials. *J. Sound Vib.* **330**, 6036–6052 (2009)
46. Cottone, F., Vocca, H., Gammaitoni, L.: Nonlinear energy harvesting. *Phys. Rev. Lett.* **102**, 080601 (2009)
47. Yan, B., Zhou, S.X., Litak, G.: Nonlinear analysis of the tristable energy harvester with a resonant circuit for performance enhancement. *Int. J. Bifurc. Chaos* **28**, 1850092 (2018)
48. Huang, D.M., Zhou, S.X., Litak, G.: Analytical analysis of the vibrational tristable energy harvester with a RL resonant circuit. *Nonlinear Dyn.* **97**, 663–677 (2019)
49. Zhou, S., Yu, T.J.: Performance comparisons of piezoelectric energy harvesters under different stochastic noises. *AIP Adv.* **10**, 035033 (2020)
50. Yang, Z.B., Erturk, A., Zu, J.: On the efficiency of piezoelectric energy harvesters. *Extreme Mech. Lett.* **15**, 26–37 (2017)
51. Adhikari, S., Friswell, M.I., Inman, D.J.: “Piezoelectric energy harvesting from broadband random vibrations. *Smart Mater. Struct.* **18**, 115005 (2009)
52. Atalik, T.S., Utku, S.: Stochastic linearization of multi-degree-of-freedom non-linear systems. *Earthq. Eng. Struct. D* **4**, 411–420 (1976)
53. Yu, T.J., Zhou, S.: Power generation mechanism and performance analysis of parametrically excited piezoelectric composite devices for vibratory energy harvesting. (2021)

Publisher's Note Springer Nature remains neutral with regard to jurisdictional claims in published maps and institutional affiliations.

Terms and Conditions

Springer Nature journal content, brought to you courtesy of Springer Nature Customer Service Center GmbH (“Springer Nature”). Springer Nature supports a reasonable amount of sharing of research papers by authors, subscribers and authorised users (“Users”), for small-scale personal, non-commercial use provided that all copyright, trade and service marks and other proprietary notices are maintained. By accessing, sharing, receiving or otherwise using the Springer Nature journal content you agree to these terms of use (“Terms”). For these purposes, Springer Nature considers academic use (by researchers and students) to be non-commercial.

These Terms are supplementary and will apply in addition to any applicable website terms and conditions, a relevant site licence or a personal subscription. These Terms will prevail over any conflict or ambiguity with regards to the relevant terms, a site licence or a personal subscription (to the extent of the conflict or ambiguity only). For Creative Commons-licensed articles, the terms of the Creative Commons license used will apply.

We collect and use personal data to provide access to the Springer Nature journal content. We may also use these personal data internally within ResearchGate and Springer Nature and as agreed share it, in an anonymised way, for purposes of tracking, analysis and reporting. We will not otherwise disclose your personal data outside the ResearchGate or the Springer Nature group of companies unless we have your permission as detailed in the Privacy Policy.

While Users may use the Springer Nature journal content for small scale, personal non-commercial use, it is important to note that Users may not:

1. use such content for the purpose of providing other users with access on a regular or large scale basis or as a means to circumvent access control;
2. use such content where to do so would be considered a criminal or statutory offence in any jurisdiction, or gives rise to civil liability, or is otherwise unlawful;
3. falsely or misleadingly imply or suggest endorsement, approval, sponsorship, or association unless explicitly agreed to by Springer Nature in writing;
4. use bots or other automated methods to access the content or redirect messages
5. override any security feature or exclusionary protocol; or
6. share the content in order to create substitute for Springer Nature products or services or a systematic database of Springer Nature journal content.

In line with the restriction against commercial use, Springer Nature does not permit the creation of a product or service that creates revenue, royalties, rent or income from our content or its inclusion as part of a paid for service or for other commercial gain. Springer Nature journal content cannot be used for inter-library loans and librarians may not upload Springer Nature journal content on a large scale into their, or any other, institutional repository.

These terms of use are reviewed regularly and may be amended at any time. Springer Nature is not obligated to publish any information or content on this website and may remove it or features or functionality at our sole discretion, at any time with or without notice. Springer Nature may revoke this licence to you at any time and remove access to any copies of the Springer Nature journal content which have been saved.

To the fullest extent permitted by law, Springer Nature makes no warranties, representations or guarantees to Users, either express or implied with respect to the Springer nature journal content and all parties disclaim and waive any implied warranties or warranties imposed by law, including merchantability or fitness for any particular purpose.

Please note that these rights do not automatically extend to content, data or other material published by Springer Nature that may be licensed from third parties.

If you would like to use or distribute our Springer Nature journal content to a wider audience or on a regular basis or in any other manner not expressly permitted by these Terms, please contact Springer Nature at

onlineservice@springernature.com